Appl Compos Mater (2018) 25:1307–1322
https://doi.org/10.1007/s10443-017-9668-7

Study on Forced Torsional Vibration of CFRP Drive-Line System with Internal Damping

Mo Yang[1] · Yefa Hu[1] · Jinguang Zhang[1] · Guoping Ding[1] · Chunsheng Song[1]

Received: 20 October 2017 / Accepted: 22 November 2017 / Published online: 3 December 2017

Abstract The use of CFRP transmission shaft has positive effect on the weight and flexural vibration reduction of drive-line system. However, the application of CFRP transmission shaft will greatly reduce the torsional stiffness of the drive-line, and may cause strong transient torsional vibration. Which will seriously affect the performance of CFRP drive-line. In this study, the forced torsional vibration of the CFRP drive-line system is carried out using the lumped parameter model. In addition, the effect of rotary inertia, internal damping, coupling due to the composite laminate, and excitation torque are incorporated in the modified transfer matrix model (TMM). Then, the modified TMM is used to predict the torsional frequency and forced torsional vibration of a CFRP drive-line with three-segment drive shafts. The results of modified TMM shown that the rotational speed difference of the CFRP transmission shaft segment is much larger than metal transmission shaft segment under excitation torque. And compared the results from finite element simulation, modified TMM and torsional vibration experiment respectively, and it has shown that the modified TMM can accurately predict forced torsional vibration behaviors of the CFRP drive-line system.

Keywords CFRP drive-line system · Forced torsional vibration · Modified transfer matrix model · Internal damping · Vibration testing

1 Introduction

A drive-line system being generally made up of several segments in series connection may generally faces challenges such as low natural frequency and large vibration. Compared with metal materials, carbon fiber reinforced plastic (CFRP) has higher specific strength, specific

✉ Mo Yang
yangmo8810@sina.cn

[1] School of Mechanical and Electronic Engineering, Wuhan University of Technology, Wuhan 430070, China

stiffness and good thermal stability [1, 2]. And replacement of any metal shaft with a CFRP transmission shaft may not only lower the mass of the drive-line system but also effectively improve the bending natural frequency of the shaft [3]. On the other hand, application of a composite transmission shaft may greatly reduce the torsional rigidity of a drive-line system. Those devices such as motors or engines may be excited by means of periodic torques so as to initiate intensive transient torsional vibration of various shaft segments; moreover, the fatigue life of the drive-line system may be seriously affected. Thus, study of excited torsional vibration of any CFRP drive-line system shall be necessarily carried out.

Currently, study of dynamic performances of composite transmission shafts focuses on those of composite shaft tubes. For example, Muslmani [4] presented analysis of the vibration of composite shafts under a transverse shear deformation or gyroscopic effect by means of Timoshenko Beam Theory. Montagnier [5] adopted Euler-Bernoulli shaft model to study the dynamic instability of supercritical drive shaft, and internal viscous or hysteretic damping were taken into account. Henry [6] studied the dynamic transverse and shear behaviors of CFRP driveshaft. Shaft self-heating model was built to evaluate the viscoelastic characterization and self-heating behavior of the CFRP shaft tube. Nezhad [7] studied nonlinear dynamics issues of composite shaft tubes under eccentric masses; moreover, he presented a comprehensive study of composite transmission shafts under bending, torsional and coupled flexure-torsion vibration effects and a multi-scale dynamic equation was established. In addition, Mutasher [8], Moorthy [9] and Quaresimin [10] studied effects of laminate parameters on the natural frequency and torsional rigidity of composite shaft tubes by means of the theory of equivalent modulus of a beam and the corresponding results indicate that growth of the laminate (0°) may not only effectively improve the natural frequency of the bending shaft but also lower its torsional rigidity. Badie [11] carried out analysis of the torsional vibration frequency of transmission shaft tubes of composite cars by means of the classical beam theory (CBT). Khalkhali [12], Cherniaev [13] and Henry [14] simplified the study object as a homogeneous simple beam for study of vibration of composite transmission shafts. All above studies may be utilized to well predict the natural frequency of bending or torsion of composite shaft tubes. However, a composite drive-line system is generally made up of several composite and metal shaft segments and its dynamic characteristics shall be the coupled results of various shaft segments, which may not be predicted by means of a dynamic model of a single composite shaft tube.

A few scholars initially focused on study of dynamic characteristics of composite shaft systems in recent years and some achievements were made. Montagnier [15] performed the optimal design of the transmission shaft of a composite helicopter under the supercritical and subcritical speeds, respectively; and effects of the composite transmission shaft, tail rotor and transmission gears were comprehensively taken into account for analysis of torsional vibration of the drive-line system so that its torsional vibration may be effectively predicted. Ding [16] performed modal analysis of a CFRP transmission shaft including metallic joints by means of the FEM method and modes were measured to obtain the results for comparison with those from related studies; and the corresponding results indicate that the metallic joints brought about great effects to the dynamic characteristics of the shaft tube. Qatu [17] studied the simple support modes of the two-segment transmission shaft of a composite car by means of the Euler-Bernoulli beam theory and composite shaft tubes and middle universal joints were taken into account in the corresponding dynamic model; and the predicted and measured natural frequencies were in good agreement. DeSmidt [18] obtained the motion equations of Flexible Matrix Composite (FMC) shaft in model order via the Finite Element Method, and explored

robust-adaptive magnetic bearing control method to ensure stable supercritical operation of a FMC driveline. All these studies of torsional vibration of composite drive-line systems were only related to prediction of the natural frequency of torsional vibration of drive-line system; on the other hand, there is rare study of the forced torsional vibration of any CFRP drive-line system under an excited torque.

Analysis of the forced torsional vibration of a composite drive-line system was carried out here by means of the lumped parameter method, whose rotational inertia, inherent dampers, coupled material stiffness and excitation torque were taken into account; moreover, an improved transfer matrix model was established to the forced torsional vibration of any composite drive-line system; in addition, the corresponding predicted and measured results were compared.

2 An Improved Transfer Matrix Model for Torsional Vibration of a CFRP Drive-Line System

As for a continuous CFRP drive-line system, it was acted by an excitation torque ($m_t(x,t)$) related to its position and time; and its torsion angle and torque were assumed as $\theta(x,t)$ and $M_T(x,t)$, respectively; moreover, a shaft element (length: $\triangle x$) may be simplified a rigid thin disk (polar moment of inertia: J_p) or a massless flexible shaft (polar moment of inertia: I_p) in Fig. 1 where the deformation and forces were presented to the i^{th} disk shaft element under the torque and the corresponding excitation; and the damping coefficient of each element is $c_i(x)$.

2.1 The Unit Transitive Relationship for a CFRP Drive-Line System

As for a rigid thin disk element (a), its rotation inertia force is $J(x)(\partial^2\theta(x,t)/\partial t^2)$ and the torque to its unit length is $\partial M_T(x,t)/\partial x$; and the following force balance equation shall be satisfied at Position x:

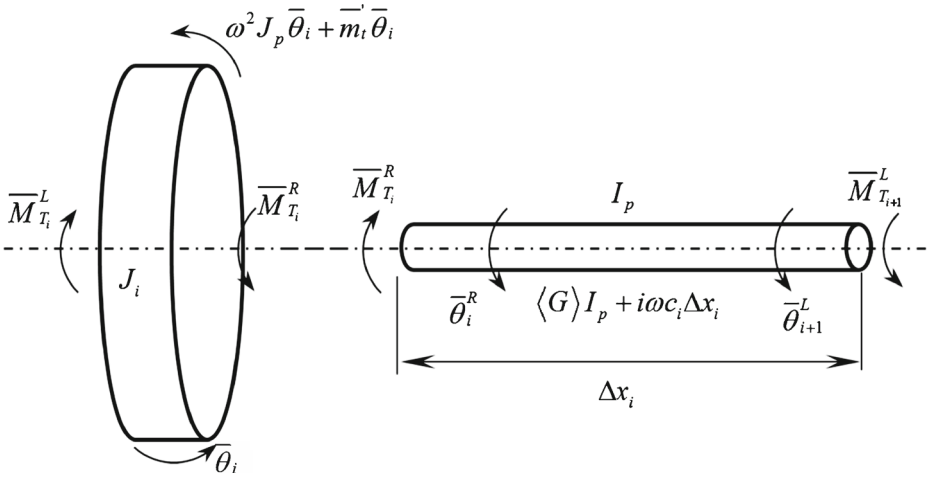

(a) The field element **(b)** Force diagram

Fig. 1 An element of a CFRP drive-line system

$$m_t(x,t) + \partial M_T(x,t)/\partial x = J(x)\left(\partial^2\theta(x,t)/\partial t^2\right) \tag{1}$$

Where: $m_t(x,t)$, $\theta(x,t)$ and $M_T(x,t)$ are variables associated with its position and time.

The corresponding harmonic function may be written as:

$$\begin{aligned} m_t(x,t) &= \overline{m}_t(x)e^{i\omega t} \\ \theta(x,t) &= \overline{\theta}(x)e^{i\omega t} \\ M_T(x,t) &= \overline{M}_T(x)e^{i\omega t} \end{aligned} \tag{2}$$

Where: $\overline{m}_t$, $\overline{\theta}$ and $\overline{M}_T$ represent the amplitudes of the excited torque, torsion angle and torque, respectively.

Integration of Eq. (2) into Eq. (1) was performed to simplify the balance equation as:

$$d\overline{M}_T(x)/dx = -\overline{m}_t(x) - J(x)\omega^2\overline{\theta}(x) \tag{3}$$

As for the rigid thin disk element, integration of $J_i \approx J(x_i)\Delta x_i$ and $\overline{m}_t \approx \overline{m}_t(x_i)\Delta x_i$ into Eq. (3) and combination of its force diagram (Fig. 1a) may result in the following equation:

$$\overline{M}_{T_i}^{R} - \overline{M}_{T_i}^{L} = -\overline{m}_t(x_i) - J(x_i)\omega^2\overline{\theta}(x_i) \tag{4}$$

Combining Eq. (4) and using the relationship $\overline{\theta}_i^R = \overline{\theta}_i^L = \overline{\theta}_i$, the transitive relationship may be obtained for the state of the i^{th} rigid thin disk element:

$$\begin{bmatrix} \overline{\theta} \\ \overline{M}_T \end{bmatrix}_i^R = \begin{bmatrix} 1 & 0 \\ -\overline{m}_t' - J_i\omega^2 & 1 \end{bmatrix} \begin{bmatrix} \overline{\theta} \\ \overline{M}_T \end{bmatrix}_i^L \tag{5}$$

Where:

$$[S]_i = \begin{bmatrix} 1 & 0 \\ -\overline{m}_t' - J_i\omega^2 & 1 \end{bmatrix} \text{ and } \overline{m}_t' = \overline{m}_t/\overline{\theta}_i$$

As for a flexible shaft element (b) and under a torque, the torsion is expressed with $\partial\theta(x,t)/\partial x$ and angular speed $(\partial\theta(x,t)/\partial t)$; and the torque shall satisfy the following balance equation:

$$M_T(x,t) = \langle G\rangle I_p(\partial\theta(x,t)/\partial x) + c_{in}(x)(\partial\theta(x,t)/\partial t) \tag{6}$$

Where: $<G>$ represents the equivalent shear modulus.

As for a metal shaft segment, its equivalent shear modulus represents the metal shear modulus.

On the other hand, the equivalent shear modulus of a composite shaft segment may be obtained based on the previous study [19]. Composite tubes are generally made by means of the positive and negative laminate alternating winding process; moreover, the mechanical analysis may be performed to minimize $\pm\varphi_i$ for discretization of laminates of a shaft tube by combining the laminate characteristics so that the coupled flexure-torsion may be eliminated; and the reduced constitutive matrix may be expressed as:

$$\begin{Bmatrix} \sigma_z \\ \sigma_\theta \\ \sigma_r \\ \tau_{\theta r} \\ \tau_{zr} \\ \tau_{z\theta} \end{Bmatrix}_{\pm\varphi} = \begin{bmatrix} \overline{Q}_{11} & \overline{Q}_{12} & \overline{Q}_{13} & 0 & 0 & 0 \\ \overline{Q}_{12} & \overline{Q}_{22} & \overline{Q}_{23} & 0 & 0 & 0 \\ \overline{Q}_{13} & \overline{Q}_{23} & \overline{Q}_{33} & 0 & 0 & 0 \\ 0 & 0 & 0 & \overline{Q}_{44} & 0 & 0 \\ 0 & 0 & 0 & 0 & \overline{Q}_{55} & 0 \\ 0 & 0 & 0 & 0 & 0 & \overline{Q}_{66} \end{bmatrix} \begin{Bmatrix} \varepsilon_z \\ \varepsilon_\theta \\ \varepsilon_r \\ \gamma_{\theta r} \\ \gamma_{zr} \\ \gamma_{z\theta} \end{Bmatrix}_{\pm\varphi} \tag{7}$$

By combining the analysis model of the torsional rigidity of a CFRP round tube, the CFRP equivalent shear modulus may be expressed as:

$$\langle G \rangle = \sum_{k=1}^{N} \left(\overline{Q}_{66}^{(k)} I_p^{(k)} \right) / I_p \tag{8}$$

The following equation may be obtained by integration of Eq. (2) into Eq. (6). And the following equation may be obtained by removal of those simple harmonic terms:

$$\overline{M}_T(x) = \langle G \rangle I_p \left(d\overline{\theta}(x)/dx \right) + i\omega c_{in}(x)\overline{\theta}(x) \tag{9}$$

The following equation may be derived based on integration of $\overline{M}_T(x) = \overline{M}_T(x_i)\Delta x_i$, $c_{in}(x) = c_{in}(x_i)\Delta x_i$ and $\overline{\theta}(x) = \left(\overline{\theta}_{i+1}^{L} - \overline{\theta}_i^{R} \right) \Delta x_i$:

$$\overline{M}_T(x_i)\Delta x_i = \left[\langle G \rangle I_p(x_j) + i\omega c_{in}(x_i)\Delta x_i \right] \left(\overline{\theta}_{i+1}^{L} - \overline{\theta}_i^{R} \right) \tag{10}$$

By combining the torque relationship ($\overline{M}_{T_i}^{\ L} = \overline{M}_{T_i}^{\ R}$) of the ith flexible shaft element, the corresponding field transitive relationship is as follows:

$$\begin{bmatrix} \overline{\theta} \\ \overline{M}_T \end{bmatrix}_{i+1}^{L} = [F]_i \begin{bmatrix} \overline{\theta} \\ \overline{M}_T \end{bmatrix}_i^{R} = \begin{bmatrix} 1 & \Delta x / \left(\langle G \rangle I_p + i\omega c_{in}\Delta x \right) \\ 0 & 1 \end{bmatrix} \begin{bmatrix} \overline{\theta} \\ \overline{M}_T \end{bmatrix}_i^{R} \tag{11}$$

2.2 The Integral Transfer Matrix of the CFRP Drive-Line System

The transfer matrix of a disc shaft element of a CFRP drive-line system may be determined by means of its state and field transitive relationships (Eqs. (5) and (11)), which is written as:

$$[T]_j = [F]_i[S]_i = \begin{bmatrix} 1 - \dfrac{\Delta x \left(\omega^2 J_i + \overline{m}_t^{'} \right)}{\left(\langle G \rangle I_p + i\omega c_{in}\Delta x \right)} & \dfrac{\Delta x}{\langle G \rangle I_p + i\omega c_{in}\Delta x} \\ -\omega^2 J_i - \overline{m}_t^{'} & 1 \end{bmatrix} \tag{12}$$

Thus, the general left-right transfer matrix of a CFRP drive-line system may be expressed as:

$$[T] = [S]_n[T]_{n-1}[T]_{n-2}\cdots[T]_2[T]_1 = \begin{bmatrix} T_{11} & T_{12} \\ T_{21} & T_{22} \end{bmatrix} \tag{13}$$

In accordance with the transitive relationships and boundary conditions and excited loads at the right and left ends of a drive-line system, analysis may be performed to its torsional vibration.

3 Solution of Torsional Vibration of a Composite Drive-Line System

The structure diagram of a drive-line system is shown in Fig. 2, where there are N + 1 rigid disc elements and N flexible shaft elements; and the natural frequency and corresponding vibration mode of its torsional vibration may be gained based on study of the free torsional vibration of a CFRP drive-line system. For obtaining the torsional vibration responses of a CFRP drive-line system under an actual excitation, analysis shall be carried out to its excited torsional vibration.

3.1 Free Torsional Vibration of a CFRP Drive-Line System

As for study of the free torsion of a drive-line system, $\overline{m}_t'$ of Eq. (12) is assumed to be 0 and its corresponding general transfer matrices may be reduced as follows:

$$[T] = [S]_N[T]_{N-1}[T]_{N-2}\cdots[T]_2[T]_1 = \begin{bmatrix} T_{11} & T_{12} \\ T_{21} & T_{22} \end{bmatrix} \tag{14}$$

Thus, the left-right transitive relationship of the torque and torsion angle of a CFRP drive-line system may be expressed as:

$$\begin{bmatrix} \overline{\theta} \\ \overline{M}_T \end{bmatrix}_{N+1}^{R} = \begin{bmatrix} T_{11} & T_{12} \\ T_{21} & T_{22} \end{bmatrix} \begin{bmatrix} \overline{\theta} \\ \overline{M}_T \end{bmatrix}_{1}^{L} \tag{15}$$

There is no any axial constraint for each end of the drive-line system under the free state so that it may be regarded as being under the free rotation state; and the corresponding boundary conditions are as follows:

$$\overline{M}_{T_1}^{L} = 0 \text{ and } \overline{M}_{T_{N+1}}^{L} = 0 \tag{16}$$

Integration of Eq. (16) into the general transitive relationship (Eq. (15)) may lead to the following simplified relationship:

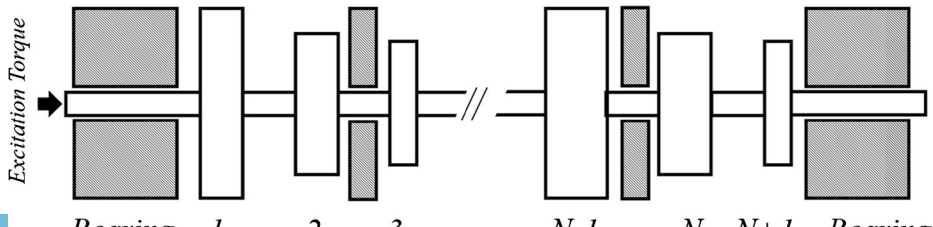

Fig. 2 Structure diagram of a CFRP drive-line system

$$\begin{cases} T_{11}\overline{\theta}_1^L - \overline{\theta}_{N+1}^R = 0 \\ T_{21}\overline{\theta}_1^L = \overline{M}_{T_{N+1}}^R = 0 \end{cases} \tag{17}$$

The non-trivial solution of the above equation requires the following equation:

$$\Delta(\omega) = \begin{vmatrix} T_{11} & -1 \\ T_{21} & 0 \end{vmatrix} = 0 \tag{18}$$

The solutions of Eq. (18) are the natural frequency (ω_n ($n = 1, 2, 3\ldots$)) of the free torsional vibration of the CFRP drive-line system.

3.2 Excited Torsional Vibration of a CFRP Drive-Line System

Due to taking the damping effects on the transfer matrix of a drive-line system and for facilitating calculation, the excited harmonic function (m_t) of the torque may be written in the complex number form, namely

$$\begin{aligned} m_t &= \overline{m}_t \cos\varphi + i\overline{m}_t \sin\varphi \\ m_t^{'} &= \overline{m}_t/\overline{\theta}\cos\varphi + i\overline{m}_t/\overline{\theta}\sin\varphi \end{aligned} \tag{19}$$

Where: φ represents the phase angle of the excitation torque; and $m_t = \overline{m}_t$ comes into existence while $\varphi = 0$; and the amplitude ($\overline{m}_t$) of the excitation torque is constant. The state transitive relationship (Eq. (5)) of a rigid thin disk may be expressed in the non-excitation and excitation torque transitive relationships as follows:

$$[S]_i = [S]_i + \left[\hat{S}\right]_i \tag{20}$$

Where: $[S]_i$ represents the non-excitation state transfer matrix; $\left[\hat{S}\right]_i$ represents the excitation torque transitive relationship; and they are written as:

$$\begin{cases} [S]_i = \begin{bmatrix} 1 & 0 \\ -J_i\omega^2 & 1 \end{bmatrix} \\ \left[\hat{S}\right]_i = \begin{bmatrix} 0 & 0 \\ -m_t^{'} & 0 \end{bmatrix} = \overline{m}_t^{'} \begin{bmatrix} 0 & 0 \\ -(\cos\varphi + i\sin\varphi) & 0 \end{bmatrix} \end{cases} \tag{21}$$

The general transitive relationship may also be described as:

$$[T] = [T] + [T] = \begin{bmatrix} T_{11} & T_{12} \\ T_{21} & T_{22} \end{bmatrix} + \begin{bmatrix} T_{11} & 0 \\ T_{21} & 0 \end{bmatrix} \tag{22}$$

The following balance equation may be got based on integration of Eq. (22) and the corresponding boundary conditions:

$$\begin{cases} (T_{11} + T_{11})\overline{\theta}_1^L - \overline{\theta}_{N+1}^R = 0 \\ (T_{21} + T_{21})\overline{\theta}_1^L = \overline{M}_{T_{N+1}}^R = 0 \end{cases} \tag{23}$$

For easy description and by taking the drive-line system shown in Fig. 2 as an example, calculation of its transfer matrix and the solution method of its excited vibration were presented as follows:

Similarly, the general transfer matrix of the drive-line system shall satisfy the following expression:

$$[T]_{(N+1)} = [S]_{N+1}[T]_N \cdots [T]_2[T]_1 + \overline{m}_t^{'}\begin{bmatrix} c_{11} & 0 \\ c_{21} & 0 \end{bmatrix} \tag{24}$$

It is known based on Eq. (24) that T_{21} is a complex number, which may be assumed as $T_{21} = (a\cos\varphi + ib\sin\varphi)\overline{m}_t^{'}$ ($\overline{m}_t^{'} = \overline{m}_t/\overline{\theta}_i$); in addition, $T_{21} = c + id$ was assumed, where a, b, c and d are constants which may be calculated based on the parameter and the transfer matrix of the drive-line system. Eq. (23) may be expressed as:

$$\left(a\cos\varphi\overline{m}_t + c\overline{\theta}_1^L\right) + i\left(b\sin\varphi + d\overline{\theta}_1^L\right) = 0 \tag{25}$$

Existence of Eq. (25) shall satisfy both the real and the imaginary parts being equal to 0. φ and $\overline{\theta}_1^L$ may be derived from Eq. (25). From this, the torsion angle, torque parameter and amplitude of excited torsional vibration of each disc shaft element may be solved by means of the general transitive relationship of the drive-line system:

$$\begin{bmatrix} \overline{\theta} \\ \overline{M}_T \end{bmatrix}_i^L = \prod_{i-1}^{1}[T]_{i-1}\begin{bmatrix} \overline{\theta} \\ 0 \end{bmatrix}_1^L, i = 2, 3\cdots N+1 \tag{26}$$

Its torque and torsion angle changes of the torsional vibration may be known based on solution of torsional vibration parameters of the CFRP drive-line system torque under any excited state; moreover, the corresponding torsional stress change may be got to provide base for study of the stability and fatigue properties of the CFRP drive-line system.

4 Free Torsional Vibration and FEM Analysis of a CFRP Drive-Line System

For verification of the reliability of the improved transfer matrix method for torsional vibration of a CFRP drive-line system described in Sections 2 and 3, our free torsional vibration study object is a three-segment composite drive-line system; and the corresponding simulated results were compared with the FEM modal analysis ones. Our CFRP drive-line system is made up of two metal transmission shaft segments and one CFRP transmission shaft segment, whose sizes are given in Table 1. As for the former, the shear modulus is G = 79Gpa; the density is 7850 kg/m^3; and the damping ratio is 0.035%. On the other hand, as for the latter, its thickness is 0.2 mm (made of T700/YPH-308 Prepregs, whose parameters are shown in Table 2); its density is 1650 kg/m^3.

The Tsai-Wu failure theory is used to assess the laminate scheme of composite tube under the maximum applied torque [20]. By comparing the torsional strength of various schemes, the laminate scheme is finally confirmed as $[\pm15°)_3/\pm45°/(\pm88°)_2/\pm45°/(\pm15°)_3/\pm88°/(\pm15°)_3/\pm45°/(\pm88°)_2/\ \pm45°/(\pm15°)_3]$. The wall thickness is 8.4 mm; and its damping ratio is 0.504%, which is calculated by the 3-D analytical model based on energy method and lamination theory [21]. In addition, the equivalent shear modulus was obtained as 16.39GPa based on the corresponding analytical method for CFRP thick round tubes (Eq. (8)).

Table 1 Section parameters of CFRP drive-line

Shaft Section No.	Length L/mm	Outer diameter D/mm	Inner diameter d/mm	Material
1	920	60	/	Metal
2	1050	59.8	43	CFRP
3	564	60	/	Metal

4.1 Analysis of Free Torsional Vibration of a CFRP Drive-Line System

Analysis was carried out to the free torsional vibration of the three-segment CFRP drive-line system by utilizing the improved transfer matrix method so that the corresponding torsional vibration natural frequency may be got. In accordance with sizes of the drive-line system in Table 1 and by combining material properties of each shaft segment, various shaft segments were discretized. The number of disc shaft elements and parameters of various disc shaft elements are given in Table 3.

By combining Eqs. (14) and (18), the general transfer matrix and residual amount ($\triangle(\omega)$) of the CFRP drive-line system under any free state were obtained; and the corresponding curve (the angular speed vs. $\triangle(\omega)$) is shown in Fig. 3. The angular speed corresponding to $\triangle(\omega) = 0$ is that of the torsional vibration of the CFRP drive-line system; and the 1st and 2nd order torsional vibration angular speeds are $\omega_1 = 1921$ rad/s and $\omega_2 = 8772$ rad/s, respectively, which corresponding torsional vibration natural frequencies are 305.89 Hz and 1396.82 Hz, respectively.

4.2 FEA (Finite Element Analysis) of a CFRP Drive-Line System

Modal simulation of the CFRP transmission drive-line system was carried out to verify the accuracy of our improved transfer matrix method for the torsional vibration of a CFRP drive-line system. The software (Abaqus 6.13) was utilized here. The sizes of our CFRP drive-line system are given in Table 1. An FEA model was established to our CFRP drive-line system; moreover, the linear perturbation analysis was carried out to obtain the natural frequency of the drive-line system. The corresponding metal part was meshed by means of the 4-node 3D–stress elements (C3D4H) as for our model; in contrast, CFRP shaft tubes were meshed by means of the 8-node 3D–stress elements (C3D8R). The analysis step was created; the analysis type was set as the analysis of frequency inside the linear perturbation; the maximum analysis modal frequency was set as 1500 Hz; and the vibration frequency of the drive-line system may be solved by submission of a job. It was found based on examination of various modal frequencies and the corresponding modal vibration modes in the analysis results that the 1st

Table 2 Material properties of CFRP T700/YPH-308

Mechanical properties	Value
E_1 longitudinal modulus /GPa	150
E_2 transverse modulus /GPa	9
G_{12} shear modulus /GPa	5.12
v_{12} Poisson's ratio	0.24

Table 3 Related parameters of our CFRP drive-line system

Shaft Segment No.	Segments	Mass /kg	Length /mm	J_p /(kg·m^2)	<GI_p> /(kg·m^2)
1	20	1.02	46.00	2.30E-04	100,464.30
2	30	0.08	35.00	2.65E-05	15,068.29
3	10	1.25	56.40	2.82E-04	100,464.30

and 2nd-order torsional vibration natural frequencies of the CFRP drive-line system were 307.95 Hz and 1426.90 Hz, respectively, whose modal vibration modes are shown in Fig. 4.

The 1st and 2nd-order torsional vibration natural frequencies of the non-excitation CFRP drive-line system were obtained by means of the improved transfer matrix and FEA methods, whose results are shown in Table 4. The improved transfer matrix method may be utilized to effectively predict torsional vibration modes of the CFRP drive-line system, as for whose predicted results the maximum deviation is only 2.11% with reference to those FEM results.

5 Vibration Tests and Excited Torsional Vibration Analysis of a CFRP Drive-Line System

Due to higher torsional vibration natural frequency of our CFRP drive-line system, the resonant angular speed may not be achieved in our drive-line system vibration test platform; thus, the excited torsional vibration of the CFRP drive-line system was measured under the subcritical rotational speed to verify the corresponding prediction accuracy of our improved transfer matrix method. The CFRP drive-line system was excited by applying a torque to a diesel engine system. The torsional vibration was measured in the middle of the CFRP transmission shaft. Measurement and calculation of the excited torsional vibration responses of the drive-line system were carried out here under various rotational speeds (900 rpm, 1000 rpm, 1100 rpm and 1200 rpm).

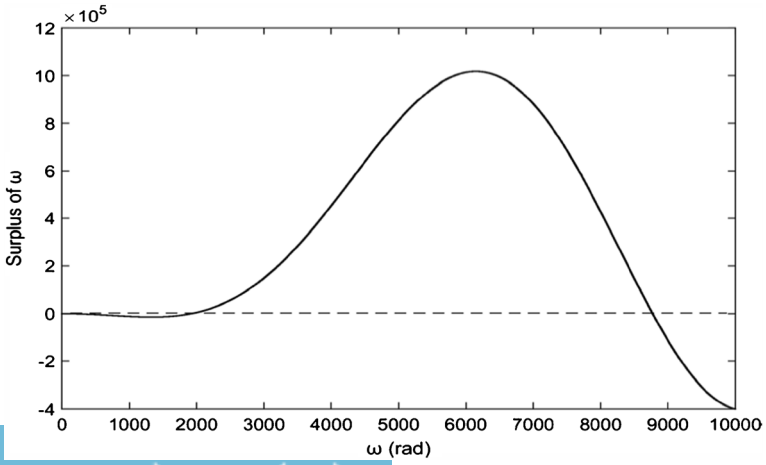

Fig. 3 Angular speed vs. $\Delta(\omega)$

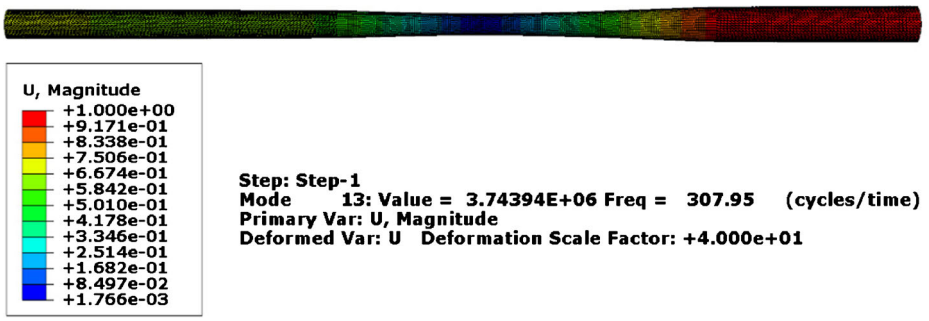

(a) 1st -order torsion modal vibration mode

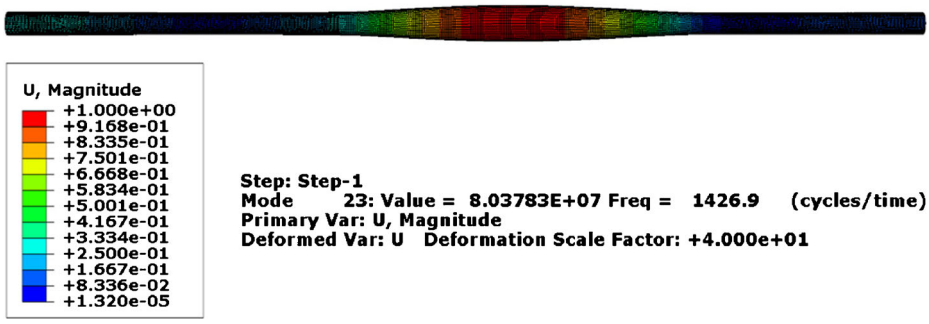

(b) 2nd -order torsion modal vibration mode

Fig. 4 Modal analysis results of our CFRP drive-line system

5.1 CFRP Drive-Line System Vibration Test Shafting Vibration Test

The CFRP drive-line system vibration measurement system is shown in Fig. 5. The strain gauge group is for measurement of the tensile strain in the angle (45°) between the CFRP transmission shaft face and the shaft line; and a data collecting card is to collect strain values for real-time data transmission by means of a wireless signal transmitter, whose sampling frequency is 4000 Hz. The shaft rotational speed is measured by means of a Hall-sensor (SS5340, SEC ELECTRONICS INC.) at the output end. A vibration test analyzer (YDZT-2013) is to receive the strain data and the corresponding vibration at the torsion angle corresponding to the measurement position is converted in accordance with parameters of our CFRP transmission shaft. Torsional vibration data of the CFRP drive-line system may be collected while a rotational speed has been stabilized. Figure 6 presents the torsional vibration curves intercepted within the period (0.5 s) under various rotational speeds.

Table 4 Comparison of results derived by means of the improved transfer matrix and FEM methods

Torsional vibration mode	Method		Deviation/%
	Modified TMM /Hz	FEA /Hz	
1	305.89	307.95	0.67
2	1396.82	1426.90	2.11

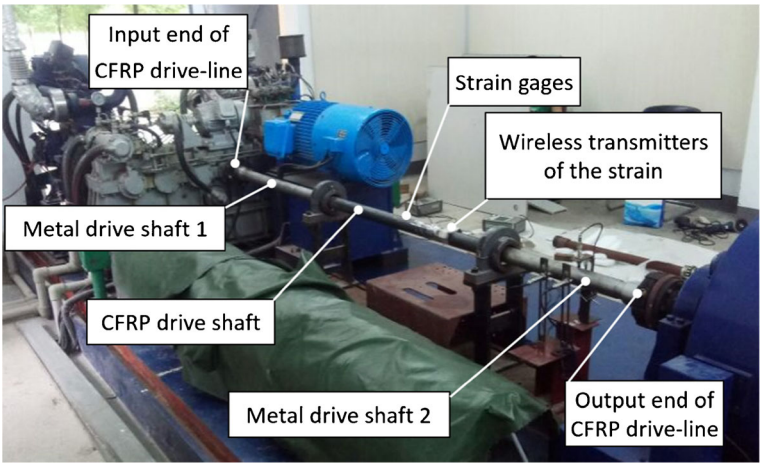

Fig. 5 CFRP drive-line system torsional vibration measurement platform

Figure 6 (torsion angle vs. rotational speed) may be utilized to obtain the amplitude of the torsional vibration corresponding to the measurement position of the drive-line system. Comparison was carried out to the measured torsional vibration results and those excited torsional vibration results derived by means of the improved transfer matrix method.

5.2 Analysis of Excited Torsional Vibration of a CFRP Drive-Line System

It was found by means of measured torque of the input end of the transmission drive-line system that excitation torque may periodically change while the diesel engine was put into operation, whose amplitude is 5% of the rated power of the diesel engine. The rated torque of the diesel engine and the excited torque amplitude at the input end of the CFRP drive-line system under each rotational speed are presented in Table 5.

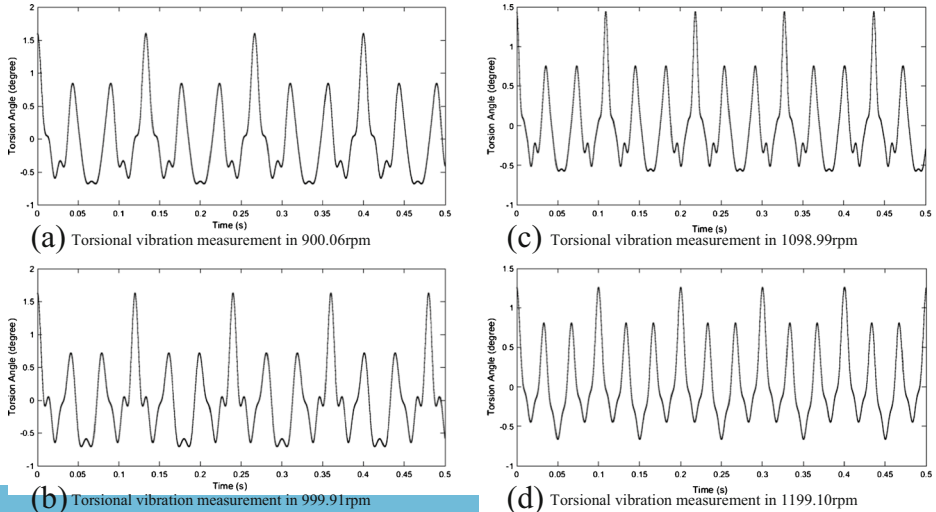

Fig. 6 Measured torsional vibration results

Table 5 Excited torsion parameters of the CFRP drive-line system

Rotational speed /rpm	Rated torque /(N·m)	Amplitude ($\overline{m}_t$) of the excitation torque /(N·m)
900.06	80	4.00
999.91	105	5.25
1098.99	110	5.50
1199.10	110	5.50

The transfer matrix under the excitation torque may be gained by integration of parameters of the disc shaft element (Table 3) and excited torque amplitudes (Table 5) in accordance with the transfer matrix method for the drive-line system; moreover, T_{21} and $\hat{T}_{21}$ may also be gained. The unknown parameters (φ and $\overline{\theta}_1^L$) of the excited vibration of the drive-line system may be solved under each rotational speed by Eq. (25).

(1) *Balance equation (n_1 = 900.06 rpm):*

$$\begin{cases} -0.994923\cos\varphi\overline{m}_t + 4.40357 \times 10^{-7} sin\varphi\overline{m}_t - 145.328\overline{\theta}_1^L = 0 \\ 4.40357 \times 10^{-7}\cos\varphi\overline{m}_t + 0.994923 sin\varphi\overline{m}_t + 3.88433 \times 10^{-5}\overline{\theta}_1^L = 0 \end{cases}$$

Solution: $\overline{\theta}_1^L$=0.0273842 *rad* and $\varphi = 3.14159$ *rad*

(2) *Balance equation (n2 = 999.91 rpm):*

$$\begin{cases} -0.99373\cos\varphi\overline{m}_t + 6.03658 \times 10^{-7} sin\varphi\overline{m}_t - 179.245\overline{\theta}_1^L = 0 \\ 6.03658 \times 10^{-7}\cos\varphi\overline{m}_t + 0.99373 sin\varphi\overline{m}_t + 6.57223 \times 10^{-5}\overline{\theta}_1^L = 0 \end{cases}$$

Solution: $\overline{\theta}_1^L$=0.0296604 *rad* and $\varphi = 3.14159$ *rad*

(3) *Balance equation (n3 = 1098.99 rpm):*

$$\begin{cases} -0.992432\cos\varphi\overline{m}_t + 8.01307 \times 10^{-7} sin\varphi\overline{m}_t - 216.374\overline{\theta}_1^L = 0 \\ 8.01307 \times 10^{-7}\cos\varphi\overline{m}_t + 0.992432 sin\varphi\overline{m}_t + 1.05395 \times 10^{-4}\overline{\theta}_1^L = 0 \end{cases}$$

Solution: $\overline{\theta}_1^L$=0.0252266 *rad* and $\varphi = 3.14159$ *rad*

(4) *Balance equation (n4 = 1199.10 rpm):*

$$\begin{cases} -0.990992\cos\varphi\overline{m}_t + 1.0406 \times 10^{-6} sin\varphi\overline{m}_t - 257.388\overline{\theta}_1^L = 0 \\ 1.0406 \times 10^{-6}\cos\varphi\overline{m}_t + 0.990992 sin\varphi\overline{m}_t + 1.62955 \times 10^{-4}\overline{\theta}_1^L = 0 \end{cases}$$

Solution: $\overline{\theta}_1^L$=0.021176 *rad* and $\varphi = 3.14159$ *rad.*

In accordance with solutions of the vibration amplitude of the left torsion angle of the 1st disc shaft element and the transitive relationship (Eq. (26)) of the CFRP drive-line system under each rotational speed, the vibration of the torsion angle may be solved for each element. The torsional vibration mode of the CFRP drive-line system

in accordance with the axial position of each element is shown in Fig. 7 for each rotational speed, where the marked position represents the vibration amplitude of the torsion angle of each position for measurement of vibration of the CFRP drive-line system. The amplitudes at the middle of the CFRP transmission shaft corresponding to each rotational speed are 1.562°, 1.660°, 1.439° and 1.208°, respectively.

The results derived by means of the improved transfer matrix method indicate that: the rules (torsional vibration vs. rotational speed) of a CFRP drive-line system under any excitation torque are consistent; namely, the difference between the rotational speeds of the metal transmission shaft segments at the both ends of the drive-line system is relatively small; on the other hand, the rotational speeds of the CFRP transmission shaft segment may changes greatly; and occurrence of such phenomena is due to the torsional rigidity of the CFRP transmission shaft being much smaller than that of the metal transmission shaft; thus, any excitation torque may more easily lead to fluctuation of the torsional vibration amplitude of the CFRP transmission shaft. As for the middle of the CFRP transmission shaft, the excited torsional vibration predicted by means of the improved transfer matrix method and the correspondingly measured results were compared.

5.3 Comparison and Discussion of Excited Vibration Results

The measured and theoretically calculated results at the sensor located in the CFRP drive-line system are given in Table 6; and the maximum deviation between the results of the amplitude of the torsional vibration obtained by means of the improved transfer matrix method and the correspondingly measured ones is 2.21%; and such case indicates that the excited torsion vibration model established by means of the improved transfer matrix method for the CFRP drive-line system may be utilized to effectively predict the excited torsional vibration; moreover, comparison of the predicted and measured torsional vibration amplitudes at the middle of the CFRP transmission shaft may show that the torsional vibration amplitude first grows and

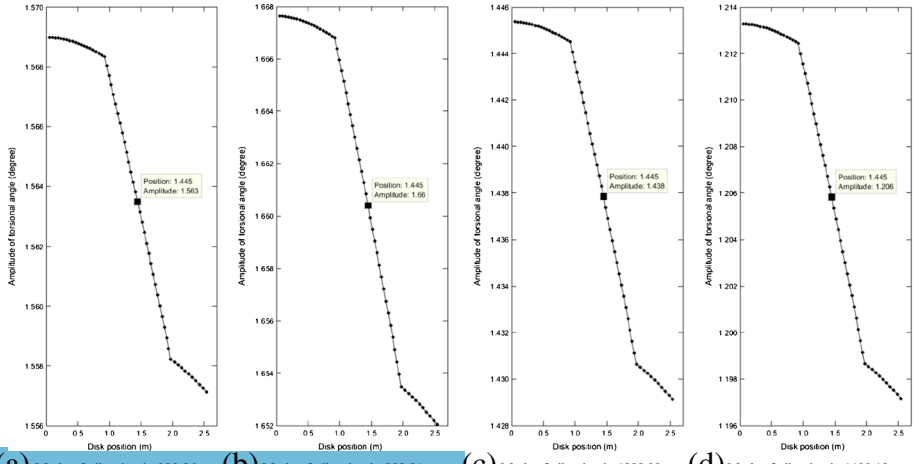

(a) Mode of vibration in 900.06rpm (b) Mode of vibration in 999.91rpm (c) Mode of vibration in 1098.99rpm (d) Mode of vibration in 1199.10rpm

Fig. 7 Excited vibration mode of the CFRP drive-line system under each rotational speed

Table 6 Comparison of the torsional vibration results derived by means of the modified TMM and correspondingly measured results

Revolving Speed/rpm	Amplitude (degree)		Deviation/%
	Modified TMM	Experiment	
900.06	1.562	1.596	2.13
999.91	1.660	1.624	2.21
1098.99	1.439	1.437	0.14
1199.10	1.208	1.205	0.25

then falls from 900.06 rpm to 1199.10 rpm so that its torsional vibration amplitude may not rise along with the growth of the rotational speed (subcritical rotational speed) or excitation torque but it may fall to a minimum under the low rotational speed, which may be regarded as a basis for analysis of the effects of the excitation torque on the torsion fatigue damage of the CFRP drive-line system.

6 Conclusions

A transfer matrix method for torsional vibration of a CFRP drive-line system was improved here based on the composite laminate theory and the lumped parameter model. A model for prediction of the torsional vibration of an excited CFRP drive-line system including inherent dampers was established. The free torsional vibration natural frequency of a three-segment CFRP drive-line system was solved by means of our improved transfer matrix model; and comparison of the corresponding results was carried out with reference to those derived by means of the FEA method; in addition, study was carried out to the method for solution of the torsional vibration responses of a CFRP drive-line system under any excitation torque; moreover, the excited vibration of the CFRP drive-line system was also measured. Comparison of results derived by means of the improved transfer matrix and FEA models and the measured vibration results may indicate the following conclusions:

- The improved transfer matrix model may be utilized to effectively predict the free torsion natural frequency of a CFRP drive-line system; and the predicted results are much consistent with those derived by means of the FEA model;
- Under excitation torque, the rotational speed difference of the CFRP transmission shaft segment is much larger than metal transmission shaft segment for a drive-line system;
- The excited torsion vibration model may be utilized to effectively predict the excited torsional vibration responses of a CFRP drive-line system, whose maximum relative deviation (between the predicted torsional vibration amplitude and the correspondingly measured ones) of the CFRP drive-line system is only 2.21%.

Acknowledgements This work supported by Research Program supported by the National Natural Science Foundation of China (No. U1537103) and the Fundamental Research Funds for the Central Universities (No. 2017-YB-017).

References

1. Gibson, R.F.: A review of recent research on mechanics of multifunctional composite materials and structures. Compos. Struct. **92**(12), 2793–2810 (2010)
2. Cho, D.H., Lee, D.G.: Manufacturing of co-cured composite aluminum shafts with compression during co-curing operation to reduce residual thermal stresses. J. Compos. Mater. **32**(12), 1221–1241 (1998)
3. Henry, T.C., et al.: Composite driveshaft prototype design and survivability testing. J. Compos. Mater. **51**(16), 2377–2386 (2017)
4. Al Muslmani, M., Ganesan, R.: Rotordynamic response of tapered composite driveshaft based on a conventional composite timoshenko finite element. 28th Annual Technical Conference of the American Society for Composites **1**, 686–705 (2013)
5. Montagnier, O., Hochard, C.: Dynamic instability of supercritical driveshafts mounted on dissipative supports—effects of viscous and hysteretic internal damping. J. Sound Vib. **305**(3), 378–400 (2007)
6. Henry, T.C., Bakis, C.E., Smith, E.C.: Viscoelastic characterization and self-heating behavior of laminated fiber composite driveshafts. Mater. Des. **66**, 346–355 (2015)
7. Shaban Ali Nezhad, H., Hosseini, S.A.A., Zamanian, M.: Flexural–flexural–extensional–torsional vibration analysis of composite spinning shafts with geometrical nonlinearity. Nonlinear Dyn. **89**(1), 651–690 (2017)
8. Mutasher, S.A.: Prediction of the torsional strength of the hybrid aluminum/composite drive shaft. Mater. Des. **30**(2), 215–220 (2009)
9. Srinivasa Moorthy, R.: Design of automobile driveshaft using carbon/epoxy and, kevlar/epoxy composites. American Journal of Engineering Research. **2**(10), 173–179 (2013)
10. Quaresimin, M., Carraro, P.A.: Damage initiation and evolution in glass/epoxy tubes subjected to combined tension–torsion fatigue loading. Int. J. Fatigue. **63**, 25–35 (2014)
11. Badie, M.A., Mahdi, E., Hamouda, A.M.S.: An investigation into hybrid carbon/glass fiber reinforced epoxy composite automotive drive shaft. Mater. Des. **32**(3), 1485–1500 (2011)
12. Khalkhali, A., Nikghalb, E., Norouzian, M.: Multi-objective optimization of hybrid carbon/glass fiber reinforced epoxy composite automotive drive shaft. Int. J. Eng. Trans. A. **28**(4), 600–609 (2015)
13. Cherniaev, A., Komarov, V.: Multistep optimization of composite drive shaft subject to strength, buckling, vibration and manufacturing constraints. Appl. Compos. Mater. **22**(5), 475–487 (2015)
14. Henry, T.C., et al.: Multi-objective optimal design of composite rotorcraft driveshaft including strain rate and temperature effects. Compos. Struct. **128**, 42–53 (2015)
15. Montagnier, O., Hochard, C.: Optimisation of hybrid high-modulus/high-strength carbon fibre reinforced plastic composite drive shafts. Mater. Des. **46**(4), 88–100 (2011)
16. Ding, G., et al.: Modal analysis based on finite element method and experimental validation on carbon fibre composite drive shaft considering steel joints. Mater. Res. Innov. **19**(S5), S5-748–S5-753 (2016)
17. Qatu, M.S., Iqbal, J.: Transverse vibration of a two-segment cross-ply composite shafts with a lumped mass. Compos. Struct. **92**(5), 1126–1131 (2010)
18. Desmidt, H.A., Wang, K.W., Smith, E.C.: Robust-adaptive magnetic bearing control of flexible matrix composite rotorcraft driveline. Journal of the American Helicopter Society. **53**(2), 115–124 (2008)
19. Hu Y., et al.: Effect of stacking sequence on the torsional stiffness of the composite drive shaft. Adv. Compos. Mater. **26**(6), 537–552 (2017)
20. Dai, G.L., et al.: Design and manufacture of an automotive hybrid aluminum/composite drive shaft. Compos. Struct. **63**(1), 87–99 (2004)
21. Tan, X., et al.: Study of the optimization of matching between torsional vibration damper and elastic coupling based on energy method. Journal of Vibroengineering. **19**(2), 769–782 (2017)